

Thermal Effects of a Couple-Stress Fluid Flow in an Elastic Tube

K. Maruthi Prasad¹, B. Sreekala^{*2}

Submitted: 05/02/2024 Revised: 11/03/2024 Accepted: 18/03/2024

Abstract: To investigate, a numerical model is suggested to analyse the effect of pliability on the peristaltic flow of a couple-stress fluid with nanoparticles in a cylindrical tube. The expressions for velocity and flux flow rate are determined by using Homotopic Perturbation method, in the process of long wave length and low Reynold's number approximations. The variation of flux is calculated by Rubinow and Keller, Muzumdar methods. The effects of different criterias on velocity and flux have been discussed. The trapping phenomena is depicted for various parameters. The flux appears to be increasing with elasticity parameters, couple-stress fluid parameter. The flux also falls as Brownian motion parameter and the Thermophoresis parameter are increased. The obtained results are same when we apply Rubinow and Keller, Muzumdar methods.

Keywords: Peristaltic flow, Elastic tube, non-Newtonian fluid, Couple-stress fluid, Volume flow rate

Introduction

The mechanism by which fluid is carried through a distensible tube when contraction or expansion waves propagate gradually throughout its length is referred to as peristalsis. From a fluid mechanics approach, peristaltic pumping is defined by the dynamical interplay of fluid flow with the movement of flexible boundaries. Peristalsis appears to be the primary mechanism for fluid transport in many physiological situations, which includes urine transport through the ureter, Intestinal chyme movement and food mixing, spermatozoa trafficking in the efferent ducts of male reproductive organs, Egg migration in the female fallopian tubes and bile duct transportation. Peristalsis is used by roller and finger pumps to push corrosive materials so that the fluid does not come into direct contact with the pump's interior surfaces. Peristalsis has been the subject of both experimental and theoretical studies. Peristalsis was first studied by Latham [1] in 1965. Unstable peristaltic transport in curved channels was explored by Ramanamurthy et al. [2]. Srinivas et al. [3] looked at the peristaltic motion of nanoparticles in a micropolar fluid in an inclined tube, as well as the effects of heat and mass transfer. Divya et al. [4] deliberated the influence of different liquid physiognomies on the peristaltic process of a convectively heated Jeffrey fluid in a greased elastic tube. Ravikumar et al. [5] analysed heat transmission and slip properties on MHD peristaltic movement of viscous fluid in a tapered microvessels. The effects of slip on the peristaltic transport of casson fluid in an inclined flexible tube

with porous walls were studied by Gudekote & Choudhari [6].

Nanofluid is a colloidal solution of nanoparticles formed when nanometer-sized particles suspended in a base fluid clash. Nanofluids often contain metals, oxides, carbides, and carbon nanotubes as nanoparticles, with water, ethylene glycol, and oil as base fluids. Microelectronics, fuel cells, pharmaceutical processes, hybrid-powered engines, engine cooling/vehicle thermal management, chiller, domestic refrigerator, and heat exchanger, as well as grinding, machining, and boiler flue gas temperature reduction, all have distinctive properties that could make nanofluids useful in a diversity of heat transfer applications. In the field of nanofluids, several studies have been undertaken and papers have been published. Choi [7] was the first to investigate nanofluid technology. Nadeem and Noreen Sher Akbar [8] investigated the flow of a micropolar fluid containing nanoparticles in small intestine. Maruthi Prasad et al. [9] investigated the peristaltic transport of a nanofluid in an inclined tube. The impact of elasticity on nanofluid peristaltic flow in a tube was investigated by Haseena et al. [10]. A computational solution for MHD peristaltic transport in an inclined nanofluid symmetric channel with porous material was provided by Abd-Alla et al. [11].

Couple-stress fluid model has been extensively used by researchers as compared to other models because of its relative mathematical intelligibility. Couple stress and spin of molecules are present in lubricants, blood with minor amounts of high

polymer additions, synthetic fluids, and electro-rheological fluids, which are not current in Newtonian fluids. As a result, for these fluids, the couple-stress fluid is a preferable model. In this field, a number of researchers have contributed. Maruthi Prasad et al. [12] investigated the peristaltic transport of a couple-stress fluid with nanoparticles in an inclined tube. The peristaltic movement of Herschel-Bulkley fluid in an unequal flexible tube was investigated by Selvi and Srinivas [13]. Srinivas Jangili et al. [14] observed couple-stress fluid flow with changeable properties: A second law analysis. Peristaltic mechanism of couple stress nanomaterial in a tapering channel has been discussed by Rafiq et al. [15].

Fluid flow in flexible tubes is fascinating because it resembles fluid movement in veins, arteries, and the urethra, among other places. Modeling elastic distortion of hollow tubes, mechanical assessment of elastic tubes used in physical therapy, cardiovascular systems to understand the evolution of pathology due to vessel contortion, and diagnostic and healing devices like pressurised

smack and prosthetic heart devices are just a few of the elastic tubes applications. Because of its importance, many studies on elastic tubes have been undertaken. Selvi and Srinivas [16] discussed the outcome of elasticity on bingham fluid flow in a tube. Sumalatha and Sreenadh [17] investigated the poiseuille flow of a jeffrey fluid in an inclined pliable tube. The peristaltic transport of a power-law fluid in a pliable tube was studied by Selvi et al. [18]. Haseena et al. [19] studied the effect of elasticity on nanofluid peristaltic flow in a tube.

Previous research has shown that while researching blood rheology in physiological systems, it is vital to take into account the tube's elastic nature. The current obstacle is to investigate the effects of elasticity on peristalsis-inducing couple stress fluid flows through a tube. In this perspective, blood is seen as pair stress fluid containing nanoparticles. The Homotopy Perturbation technique is used to solve the temperature profile and nano particle phenomena. Graphs are used to analyse the results of analytic equations for flow quantities.

Mathematical Formulation

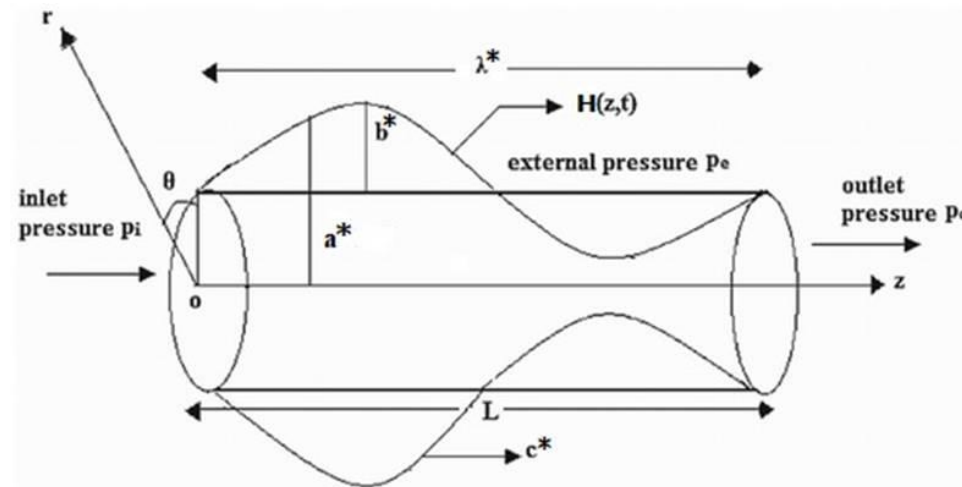


Fig. 1. Peristaltic Transport of a Couple –Stress Fluid in an Elastic tube

Consider the peristaltic transport of a nanoparticle-containing incompressible couple stress fluid in a tube with a uniform cross section of radius a^* , amplitude b^* , wave length λ^* , and a sinusoidal wave travelling along the tube's boundary at c^* . The physical model with cylindrical coordinate system (R, θ, Z) is shown below.

$$T_{ij,j} = \rho \frac{dw_i}{dt} \quad (2)$$

The deformation of the wall is written as

$$R = H(z, t) = a^* + b^* \sin \frac{2\pi}{\lambda^*} (Z - c^*t) \quad (1)$$

In the absence of body couple and body moment, the required governing equations for this situation are as follows [12]

$$e_{ijk}T_{jk}^A + M_{ji,j} = 0 \quad (3)$$

$$l_{ij} = -p\delta_{ij} + 2\mu_{ij}d_{ij} \quad (4)$$

$$\mu_{ij} = 4\eta\omega_{j,i} + 4\eta'\omega_{ij} \quad (5)$$

$$(\rho c)_f \frac{dT'}{dt} = k\nabla^2 T' + (\rho c)_p \left[D_B \nabla C' \cdot \nabla T' + \frac{D_T}{T_0'} \nabla T' \cdot \nabla T' \right] \quad (6)$$

$$\frac{dc'}{dt} = D_B \nabla^2 C' + \left[\frac{D_T'}{T_0'} \right] \nabla^2 T' \quad (7)$$

Here w_i is the velocity vector, T_{ij} and T_{ij}^A are the symmetric and antisymmetric parts of the tensor T_{ij} , M_{ij} is the couple-stress tensor, μ_{ij} is the deviatoric part of M_{ij} , ω_{ij} is the vorticity vector, d_{ij} is the symmetric part of the velocity gradient, and η and η' are constants associated with the couple-stress. The density of the fluid is ρ_f ,

Making use of the transformation

$$r = R, z = Z - c^*t, u = U, w = W - c^*, \theta = \theta$$

Equations (2) to (7) are translated from a stationary to a moving frame of reference

$$\mu \nabla^2 \left[1 - \frac{1}{\bar{\alpha}^2} \nabla^2 \right] w' = \frac{dp'}{dz'} + \rho g \beta (T' - T_0) + \rho g \beta (C' - C_0) \quad (8)$$

$$\left[u' \frac{\partial T'}{\partial r'} + w' \frac{\partial T'}{\partial z'} \right] = \beta \left[\frac{\partial^2 T'}{\partial r'^2} + \frac{1}{r'} \frac{\partial T'}{\partial r'} + \frac{\partial^2 T'}{\partial z'^2} \right] + \tau \left\{ D_B \left[\frac{\partial C'}{\partial r'} \frac{\partial T'}{\partial r'} + \frac{\partial C'}{\partial z'} \frac{\partial T'}{\partial z'} \right] + \frac{D_T'}{T_0'} \left[\left(\frac{\partial T'}{\partial r'} \right)^2 + \left(\frac{\partial T'}{\partial z'} \right)^2 \right] \right\} \quad (9)$$

$$\left[u' \frac{\partial C'}{\partial r'} + w' \frac{\partial C'}{\partial z'} \right] = D_B \left[\frac{\partial^2 C'}{\partial r'^2} + \frac{1}{r'} \frac{\partial C'}{\partial r'} + \frac{\partial^2 C'}{\partial z'^2} \right] + \frac{D_T'}{T_0'} \left[\frac{\partial^2 T'}{\partial r'^2} + \frac{1}{r'} \frac{\partial T'}{\partial r'} + \frac{\partial^2 T'}{\partial z'^2} \right] \quad (10)$$

Where $\nabla^2 = \frac{1}{r} \frac{\partial}{\partial r} \left(r \frac{\partial}{\partial r} \right)$ and $\tau = \frac{(\rho c)_p}{(\rho c)_f}$ is the ratio of the nanoparticle material's effective heat capacity to the fluid's heat capacity.

Introducing the non-dimensional quantities listed below:

$$r = \frac{r'}{a^*}, z = \frac{z'}{\lambda^*}, w = \frac{w'}{c^*}, p = \frac{a^* p'}{\lambda^* c^* \mu}, t = \frac{c^* t'}{\lambda^*}, u = \frac{\lambda^* u'}{a^* c^*}, \theta_t = \frac{T' - T_0'}{T_0'}, \delta = \frac{a^*}{\lambda^*}, Re = \frac{2\rho c^* a^*}{\mu},$$

$$\sigma = \frac{C' - C_0'}{C_0'}, \beta = \frac{k}{(\rho c)_f}, N_b = \frac{(\rho c)_p D_B C_0'}{(\rho c)_f}, N_t = \frac{(\rho c)_p D_T T_0'}{(\rho c)_f \beta}, G_r = \frac{g \beta a^3 T_0'}{\gamma^2}, B_r = \frac{g \beta a^3 C_0'}{\gamma^2},$$

$$\bar{\alpha} = a^* \alpha = \sqrt{\frac{\mu}{\eta}} a^*, h' = \frac{h}{a^*}$$

Equations (8) – (10) are transformed to (11) – (13) by using long wavelength and low Reynolds

$$\frac{1}{r} \frac{\partial}{\partial r} \left(r \frac{\partial}{\partial r} \left(1 - \frac{1}{\bar{\alpha}^2} \nabla^2 \right) w \right) = \frac{dp}{dz} + G_r \theta + B_r \sigma \quad (11)$$

$$0 = \frac{1}{r} \frac{\partial}{\partial r} \left(r \frac{\partial \theta}{\partial r} \right) + N_b \frac{\partial \sigma}{\partial r} \frac{\partial \theta}{\partial r} + N_t \left(\frac{\partial \theta}{\partial r} \right)^2 \quad (12)$$

$$0 = \frac{1}{r} \frac{\partial}{\partial r} \left(r \frac{\partial \sigma}{\partial r} \right) + \frac{N_t}{N_b} \left(\frac{1}{r} \frac{\partial}{\partial r} \left(r \frac{\partial \theta}{\partial r} \right) \right) \quad (13)$$

Where N_b , N_t , G_r , B_r , w , r , $\bar{\alpha}$, θ and σ are Brownian motion parameter, Thermophoresis parameter, Local temperature Grashof number,

particle density is ρ_p , volumetric volume expansion coefficient is C , body forces are f , $\frac{d}{dt}$ is material time derivative, nano particle concentration is \bar{C} , Brownian diffusion coefficient is D_B , and thermophoretic diffusion coefficient is D_T . \bar{T} and \bar{C} ambient values as \bar{r} tend to \bar{h} are represented by \bar{T}_0 and \bar{C}_0 , respectively.

number approximation, the dimensionless equations after removing bars can be written as

Local nanoparticle Grashof number, axial velocity, radial coordinate, couple-stress fluid parameter,

temperature profile and nanoparticle phenomenon respectively.

The dimensionless boundary conditions are as follows:

$$\begin{cases} \frac{\partial w}{\partial r} = 0, \frac{\partial \theta}{\partial r} = 0, \frac{\partial \sigma}{\partial r} = 0 & \text{at } r = 0 \\ w = -1, \theta = 0, \sigma = 0 & \text{at } r = h(z) = 1 + \epsilon \sin 2\pi z \\ \frac{\partial^2 w}{\partial r^2} - \frac{\eta}{r} \frac{\partial w}{\partial r} = 0 & \text{at } r = h(z) = 1 + \epsilon \sin 2\pi z \\ \frac{\partial^2 w}{\partial r^2} - \frac{\eta}{r} \frac{\partial w}{\partial r} \text{ is finite} & \text{at } r = 0 \end{cases} \quad (14)$$

The amplitude ratio is $\epsilon = \left(\frac{b^*}{a^*}\right)$ and $\eta' = \frac{\eta}{\eta}$ is couple-stress fluid parameter

Couple-stress vanishes in the tube wall and becomes finite at the tube axis, according to the last two boundary conditions (14)

Solution of the problem

The Homotopy Perturbation method (HPM) combines Homotopy and Perturbation methods. The HPM is a better choice than the other classic perturbation methods. We shall be able to overcome the disadvantages of classic perturbation methods by employing this strategy.

The following are homotopy equations for (12) and (13) as (He JH, [20])

$$H(q, \theta) = L(\theta) - L(\theta_{10}) + qL(\theta_{10}) + q \left[N_b \frac{\partial \sigma}{\partial r} \frac{\partial \theta}{\partial r} + N_t \left(\frac{\partial \theta}{\partial r} \right)^2 \right] \quad (15)$$

$$H(q, \sigma) = L(\sigma) - L(\sigma_{10}) + qL(\sigma_{10}) + q \left[\frac{N_t}{N_b} \frac{1}{r} \frac{\partial}{\partial r} \left(r \frac{\partial \theta}{\partial r} \right) \right] \quad (16)$$

For convenience, $L = \frac{1}{r} \frac{\partial}{\partial r} \left(r \frac{\partial}{\partial r} \right)$ is used as the linear operator

$$\theta_{10}(r, z) = \left(\frac{r^2 - h^2}{4} \right), \sigma_{10}(r, z) = - \left(\frac{r^2 - h^2}{4} \right) \quad (17)$$

Equation(17) described as initial guesses which satisfy the boundary conditions.

Define

$$\theta(r, z) = \theta_0 + q\theta_1 + q^2\theta_2 + \dots \quad (18)$$

$$\sigma(r, z) = \sigma_0 + q\sigma_1 + q^2\sigma_2 + \dots \quad (19)$$

For the most part, the series (18) and (19) are convergent. The nonlinear part of the equation determines the convergence rate.

Analysis for temperature and nano particle phenomena is stated as for $q = 1$ using same technique as (He JH, [20])

$$\theta(r, z) = N_b(N_b - N_t) \left(\frac{r^6 - h^6}{1152} \right) - N_t(N_b - N_t) \left(\frac{r^6 - h^6}{576} \right) - (N_b - 2N_t) \left(\frac{r^4 - h^4}{64} \right) \quad (20)$$

$$\sigma(r, z) = - \frac{N_t}{N_b} (N_b - N_t) \left(\frac{r^4 - h^4}{64} \right) \quad (21)$$

Substituting equations (20) and (21) in equation (11), can be written as

$$\frac{1}{r} \frac{\partial}{\partial r} \left(r \frac{\partial}{\partial r} \left(1 - \frac{1}{\bar{\alpha}^2} \nabla^2 \right) w \right) = \frac{dp}{dz} + G_r \left\{ N_b(N_b - N_t) \left(\frac{r^6 - h^6}{1152} \right) - N_t(N_b - N_t) \left(\frac{r^6 - h^6}{576} \right) - (N_b - 2N_t) \left(\frac{r^4 - h^4}{64} \right) \right\} + B_r \left\{ - \frac{N_t}{N_b} (N_b - N_t) \left(\frac{r^4 - h^4}{64} \right) \right\} \quad (22)$$

The expression for velocity is found by solving Eq. (22) applied to the boundary conditions (14)

$$\begin{aligned} w = & -1 + S_1 [I_0(\bar{\alpha}r) - I_0(\bar{\alpha}h)] + \frac{dp}{dz} \left[\frac{r^2 - h^2}{4} - \frac{(1-\eta)}{2A} (I_0(\bar{\alpha}r) - I_0(\bar{\alpha}h)) \right] + G_r N_b (N_b - N_t) \left[\frac{r^6 - h^6}{1152(\bar{\alpha})^2} + \frac{r^4 - h^4}{32(\bar{\alpha})^4} + \right. \\ & \left. \frac{r^2 - h^2}{2(\bar{\alpha})^6} - \frac{r^2 h^6}{4608} + \frac{r^8}{73728} + \frac{5h^8}{24576} \right] + G_r N_t (N_b - N_t) \left[- \frac{(r^6 - h^6)}{1152(\bar{\alpha})^2} - \frac{(r^4 - h^4)}{16(\bar{\alpha})^4} - \frac{(r^2 - h^2)}{(\bar{\alpha})^6} + \frac{r^2 h^6}{2304} - \frac{r^8}{36864} - \frac{5h^8}{12288} \right] + \\ & G_r (N_b - 2N_t) \left[- \frac{(r^4 - h^4)}{64(\bar{\alpha})^2} - \frac{(r^2 - h^2)}{4(\bar{\alpha})^4} + \frac{r^2 h^4}{256} - \frac{r^6}{2304} - \frac{h^6}{288} \right] + B_r \frac{N_t}{N_b} (N_b - N_t) \left[- \frac{(r^4 - h^4)}{64(\bar{\alpha})^2} - \frac{(r^2 - h^2)}{4(\bar{\alpha})^4} + \frac{r^2 h^4}{256} - \frac{r^6}{2304} - \frac{h^6}{288} \right] \quad (23) \end{aligned}$$

Where $A = \bar{\alpha} \left[\bar{\alpha} I_0(\bar{\alpha}h) - \frac{(1+\bar{\eta})}{h} I_1(\bar{\alpha}h) \right]$

$$S_1 = \left\{ -G_r N_b (N_b - N_t) \left[\frac{(1+\bar{\eta})h^6}{3072} + \frac{(1-\bar{\eta})}{\bar{\alpha}^6} + \frac{(3-\bar{\eta})h^2}{8\bar{\alpha}^4} + \frac{h^4}{192} \left(5 - \frac{\bar{\eta}}{\bar{\alpha}^2} \right) \right] \right. \\ - G_r N_t (N_b - N_t) \left[-\frac{(1+\bar{\eta})h^6}{1536} + \frac{(\bar{\eta}-5)h^4}{96\bar{\alpha}^2} + \frac{(\bar{\eta}-3)h^2}{4\bar{\alpha}^4} + \frac{2(\bar{\eta}-1)}{\bar{\alpha}^6} \right] \\ - G_r (N_b - N_t) \left[-\frac{(1+\bar{\eta})h^4}{192} + \frac{(\bar{\eta}-1)}{2\bar{\alpha}^4} + \frac{h^2(\bar{\eta}-3)}{16\bar{\alpha}^2} \right] \\ \left. - B_r \frac{N_t}{N_b} (N_b - N_t) \left[-\frac{(1+\bar{\eta})h^4}{192} + \frac{(\bar{\eta}-1)}{2\bar{\alpha}^4} + \frac{h^2(\bar{\eta}-3)}{16\bar{\alpha}^2} \right] \right\} / A$$

In the moving frame, the dimension less flux is given as

$$Q = \int_0^h r w \, dr \tag{24}$$

Substituting equation (23) in equation (24) and solving, the flux is

$$Q = P S_0 + F \tag{25}$$

Where

$$F = -h^2 + 2S_1 S + G_r N_b (N_b - N_t) \left[\frac{h^{10}}{10240} - \frac{h^8}{1536\bar{\alpha}^2} - \frac{h^6}{48\bar{\alpha}^4} - \frac{h^4}{4\bar{\alpha}^6} \right] + G_r N_t (N_b - N_t) \left[-\frac{h^{10}}{5120} + \frac{h^8}{1536\bar{\alpha}^2} + \frac{h^6}{24\bar{\alpha}^4} + \frac{h^4}{2\bar{\alpha}^6} \right] \\ + G_r (N_b - 2N_t) \left[-\frac{5h^8}{3072} + \frac{h^6}{96\bar{\alpha}^2} + \frac{h^4}{8\bar{\alpha}^4} \right] + B_r \frac{N_t}{N_b} (N_b - N_t) \left[-\frac{5h^8}{3072} + \frac{h^6}{96\bar{\alpha}^2} + \frac{h^4}{8\bar{\alpha}^4} \right]$$

$$S = h I_1(\bar{\alpha}h) - \frac{h^2}{2} I_0(\bar{\alpha}h)$$

$$S_0 = -\frac{(\bar{\eta}-1)}{A} S + \frac{h^4}{8} \text{ and } P = -\frac{dp}{dz}$$

Theoretical Determination of Flux

To find the flux of couple-stress fluid through an elastic tube, Rubinow and Keller method was applied [22]. Let p_0 represent the external pressure and p_1 and p_2 represent the fluid pressures at the entrance and exit, respectively. The pressure at the entrance, p_1 , is expected to be higher than the

$$Q = \sigma(p - p_0)(P + F) \tag{26}$$

Where $\sigma(p - p_0) = S_0$

Using the inlet condition and from $z = 0$, integrating equation (26) with respect to z

$p(0) = p_1$, we obtain

$$Q_z = \int_{p(z)-p_0}^{p_1-p_0} \sigma(p') \, dp' + \int_0^z S_0 \, dz \tag{27}$$

$p' = p(z) - p_0$ in this case. Equation (21) gives $p(z)$, in terms of Q and z . By substituting $z=1$ and $p(1) = p_2$ into the equation (27), we get Q.

$$Q_z = \int_{p(1)-p_0}^{p_1-p_0} \sigma(p') \, dp' + \int_0^z S_0 \, dz \tag{28}$$

In this instance, where $h = h(p - p_0)$

On the other hand, Equation (28) can be written as

$$Q = \int_{p_2-p_0}^{p_1-p_0} S_0 \, dp' + F S_0 \tag{29}$$

pressure at the exit, p_2 . The tube wall can expand or shrink as the pressure within and outside the tube changes. Pressure variance affects the conductivity of the tube at z . As a result, the conductivity function $\sigma = \sigma[p(z) - p_0]$ is equal to $(p(z) - p_0)$. The expression also relates the flow Q and the pressure gradient.

The equilibrium condition determines $h(p - p_0)$, If the tension or stress $T(h)$ in the tube wall is also

$$\frac{T(h)}{h} = p - p_0 \quad (30)$$

Method of Rubinow and Keller

Static pressure-volume relationship of a 4cm section of human external artery is translated to a

$$T(h) = t_1(h - 1) + t_2(h - 1)^5$$

When we use (31) in place of (30), we get

$$dp' = \left[\frac{t_1}{h^2} + t_2 \left(4h^3 - 15h^2 + 20h - 10 + \frac{1}{h^2} \right) \right] dh \quad (32)$$

where $t_1 = 13$ and $t_2 = 300$

Equation (29) can be written as, using equation (32)

$$Q = \int_{p_2-p_0}^{p_1-p_0} S_0 \left[\frac{t_1}{h^2} + t_2 \left(4h^3 - 15h^2 + 20h - 10 + \frac{1}{h^2} \right) \right] dh + F(h(p_2 - p_0)^4) \quad (33)$$

Flux is simplified even further

$$Q = g(h_1) - g(h_2) + Fh_2^4$$

Where $g(h) = t_1 \left(-\frac{S_0}{h} \right) + t_2 \left(h^4 - 5h^3 + 10h^2 - 10h - \frac{1}{h} \right) S_0$

$$h_1 = h(p_1 - p_0)$$

$$h_2 = h(p_2 - p_0) \quad (34)$$

Method of Mazumdar

The tension relationship can be written as follows, according to Mazumdar [21]

$$T(h) = A(e^{kh} - e^k) \quad (35)$$

By substituting Eq. (35) in Eq. (30) for $A = 0.007435$ and $k = 5.2625$, we get

$$p - p_0 = A \left[\frac{e^{Kh}}{h} - \frac{e^K}{h} \right]$$

$$dp' = A \left[e^{Kh} \left(\frac{K}{h} - \frac{1}{h^2} \right) + \frac{e^K}{h^2} \right] dh \quad (36)$$

We get the flux by putting Eq. (36) into Eq. (29)

$$Q = \int_{p_2-p_0}^{p_1-p_0} S_0 A \left[e^{Kh} \left(\frac{K}{h} - \frac{1}{h^2} \right) + \frac{e^K}{h^2} \right] dh + F(h(p_2 - p_0)^4)$$

Where $h = h(p - p_0)$

$$Q = \frac{1}{8} [(g(h_1) - g(h_2))] + Fh_2^4 \quad (37)$$

Where $g(h) = \frac{e^{kh}}{k^3} (h^3 k^3 - 4h^2 k^2 + 8hk - 8) + e^k \frac{h^3}{3}$

Results and Discussions

The effect of elasticity on peristaltic pumping may have several biological applications in the design of artificial pumps. It is a natural phenomenon observed in every living system. In the present article we considered two types of phenomenon one is elasticity and other one is couple-stress fluid.

called a function of h .

tension against length curve and applied to arterial flow. Using the least-squares method, Rubinow and Keller [22] developed the following equation.

$$(31)$$

(32)

$$(33)$$

(34)

$$(35)$$

(36)

$$(37)$$

(38)

(39)

(40)

(41)

(42)

(43)

(44)

(45)

(46)

(47)

(48)

(49)

(50)

The knowledge pertaining to elasticity with different Non-newtonian fluids have many industrial applications.

The flow pattern of peristaltic blood transport in an elastic tube is examined in this work. Blood is used as a couple-stress fluid here. Change in fluid flux for various physiological parameters such as

couple-stress fluid parameters $(\bar{\alpha}, \bar{\eta})$, Brownian motion parameter (N_b) , Thermophoresis parameter (N_t) , Local temperature Grashof number (G_r) , and local nanoparticle Grashof number (B_r) was detailed and graphically represented in this paper. Mathematica is used to create the graphs.

Figures 2 to 9 shows the variation in volume flow rate using Rubinow and Keller method for different parameters.

The effect of elastic parameters t_1 and t_2 on flux variation is found from Figs. 2 and 3 respectively. That is with increasing values of elastic radius parameters promotes the flux in elastic tube i.e., when the radius of the tube increases then collision between the molecules also upsurges resulting in increase of the flux.

Figures 4 and 5 illustrate the flux decreases with increasing values of Brownian motion

parameter (N_b) and Thermophoresis parameter (N_t) . It is interesting to note that in figure 4, values are constant for shorter period of time and further the flux decreases along the tube radius is more than 6.5.

Figures 6 and 7 shows the variation of flux rise with respect to radius. It is clear that the flux increased with increase of Local temperature Grashof number (G_r) and local nanoparticle Grashof number (B_r) . It is observed from the fig.7 shows a constant value upto radius 7 and it starts to decline later.

The flux along tube radius for numerous values of couple-stress fluid is shown in figures 8 and 9. It is evident that the increasing values of couple-stress fluid increases the flux variation.

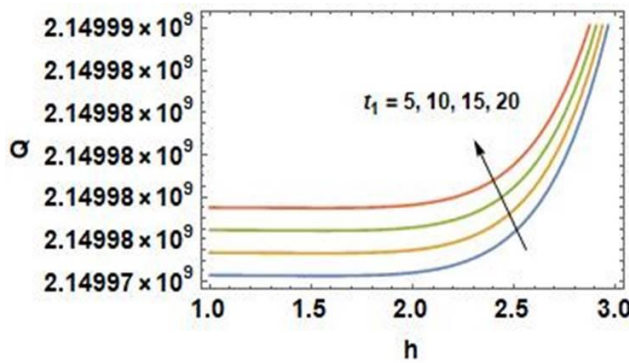


Fig. 2. Flux Q vs. radius h with elastic parameter t_1 for $t_2 = 100, N_b = 12, N_t = 20, G_r = 8, B_r = 20, \alpha = 2.2, \eta = 0.8$ (Rubinow and Keller)

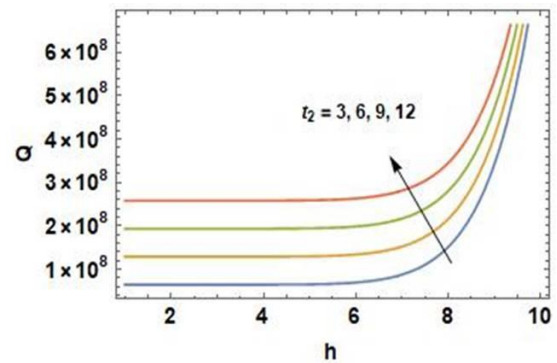


Fig. 3. Flux Q vs. radius h with elastic parameter t_2 for $t_1 = 50, N_b = 9, N_t = 15, G_r = 6, B_r = 15, \alpha = 2.2, \eta = 0.8$ (Rubinow and Keller)

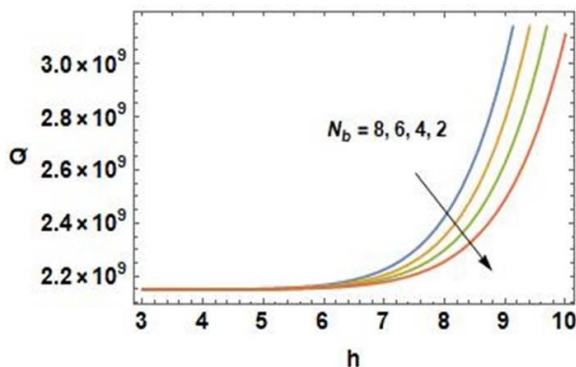


Fig. 4. Flux Q vs. radius h with Brownian motion parameter N_b for $t_1 = 50, t_2 = 100, N_t = 15, G_r = 6, B_r = 15, \alpha = 2.2, \eta = 0.8$ (Rubinow and Keller)

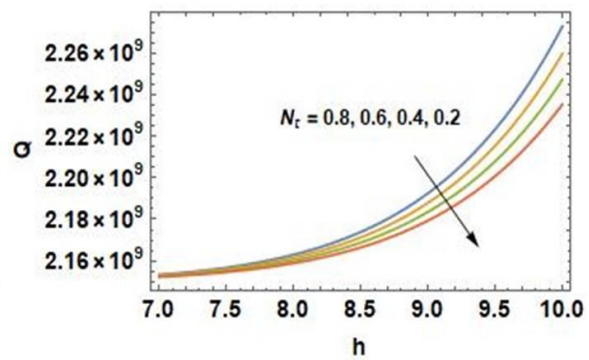


Fig. 5. Flux Q vs. radius h with Thermophoresis parameter N_t for $t_1 = 50, t_2 = 100, N_b = 6, G_r = 4, B_r = 10, \alpha = 2.2, \eta = 0.8$ (Rubinow and Keller)

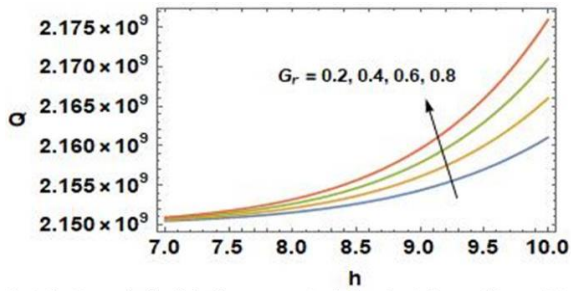


Fig. 6. Flux Q vs. radius h with local temperature Grashof number G_r , for $t_1 = 50, t_2 = 100, N_b = 2, N_t = 5, B_r = 5, \alpha = 2.2, \eta = 0.8$ (Rubinow and Keller)

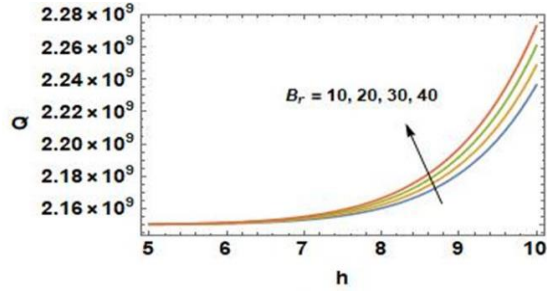


Fig. 7. Flux Q vs. radius h with local nanoparticle Grashof number B_r , for $t_1 = 50, t_2 = 100, N_b = 2, N_t = 5, G_r = 3, \alpha = 2.2, \eta = 0.8$ (Rubinow and Keller)

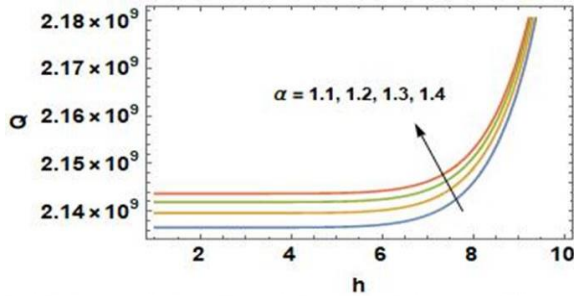


Fig. 8. Flux Q vs. radius h with couple-stress fluid parameter α for $t_1 = 50, t_2 = 100, N_b = 2, N_t = 5, G_r = 3, B_r = 5, \eta = 0.8$ (Rubinow and Keller)

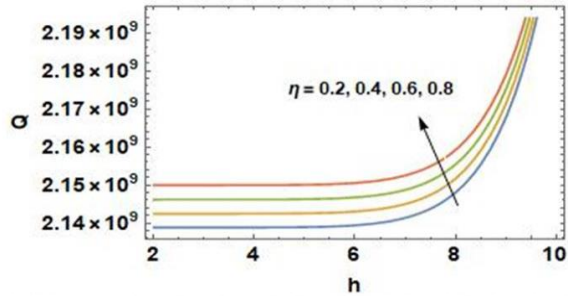


Fig. 9. Flux Q vs. radius h with couple-stress fluid parameter η for $t_1 = 50, t_2 = 100, N_b = 2, N_t = 5, G_r = 3, B_r = 5, \alpha = 2.2$ (Rubinow and Keller)

The similar behaviour is observed from Figures 10 to 17 shows the variation in volume flow rate using Mazumdar method for different parameters.

Figures 10 and 11 show that the flux increases as the elastic parameters K and A increase. In particular the elastic parameter K shows more effect on the flux when compared to A .

Figures 12 and 13 illustrate the flux variation along tube radius for change in standards of Brownian motion parameter (N_b) and Thermophoresis parameter (N_t). With rising levels of N_b and N_t , the volume flow rate clearly drops. It is also interesting to note that in figure 12 and 13, values are constant for shorter period of time and further the flux decreases along the tube radius is more than 2.

Figures 14 and 15 show the flux fluctuation around the radius for various values of the local temperature Grashof number (G_r) and local nanoparticle Grashof number (B_r). It represents that the flux increases for increasing G_r values whereas it increases with increasing B_r values. It is noticed from figures 14 and 15 shows a constant value upto radius 2 and it starts to decline later.

Figures 16 and 17 represents, flux variation along radius of the elastic tube for different couple-stress fluid numbers. From these graphs, one can see the increase in couple-stress fluid increase flux for different values.

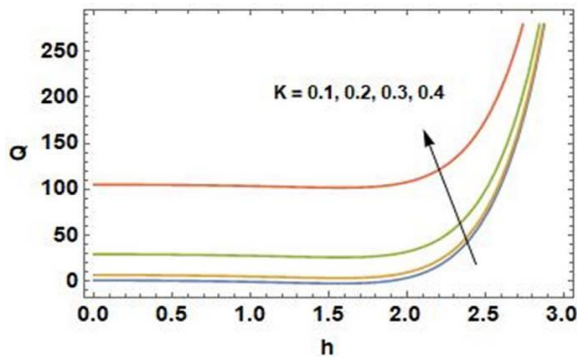


Fig. 10. Flux Q vs. radius h with elastic parameter K for $A = 0.0074, N_b = 3, N_t = 5, G_r = 2, B_r = 5, \alpha = 2.2, \eta = 0.8$ (Mazumdar method)

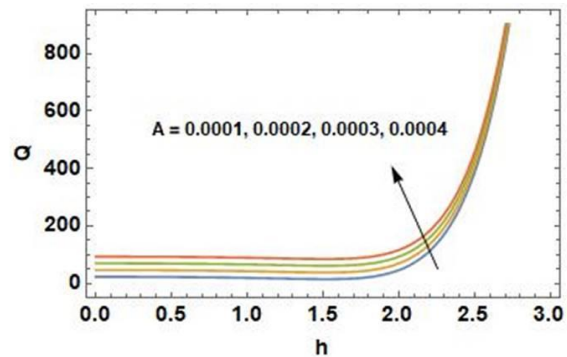


Fig. 11. Flux Q vs. radius h with elastic parameter A for $K = 5.26, N_b = 6, N_t = 10, G_r = 4, B_r = 10, \alpha = 2.2, \eta = 0.8$ (Mazumdar method)

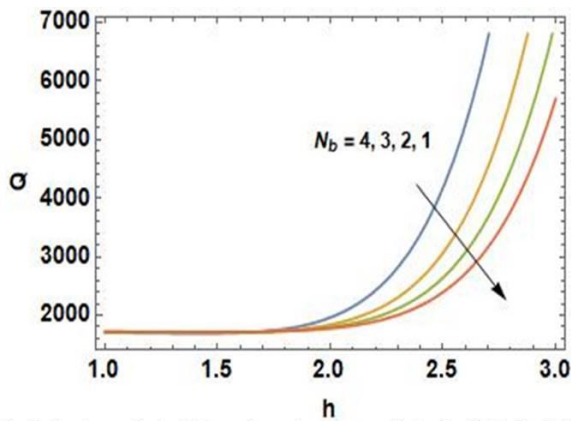


Fig. 12. Flux Q vs. radius h with Brownian motion parameter N_b for $K = 5.26$, $A = 0.0074$, $N_t = 10$, $G_r = 4$, $B_r = 10$, $\alpha = 2.2$, $\eta = 0.8$ (Mazumdar method)

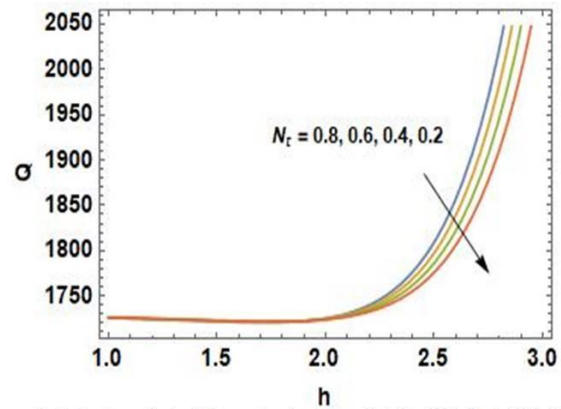


Fig. 13. Flux Q vs. radius h with Thermophoresis parameter N_t for $K = 5.26$, $A = 0.0074$, $N_b = 6$, $G_r = 4$, $B_r = 10$, $\alpha = 2.2$, $\eta = 0.8$ (Mazumdar method)

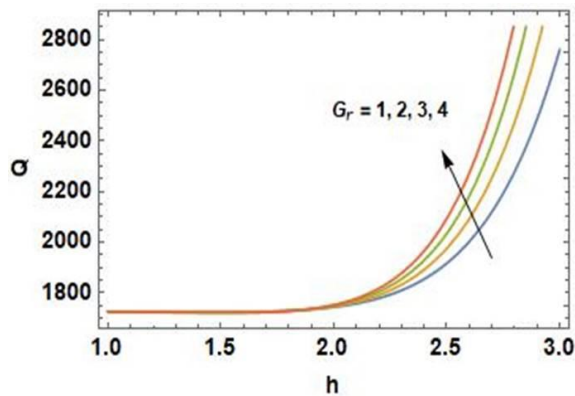


Fig. 14. Flux Q vs. radius h with local temperature Grashof number G_r for $K = 5.26$, $A = 0.0074$, $N_b = 6$, $N_t = 10$, $B_r = 10$, $\alpha = 2.2$, $\eta = 0.8$ (Mazumdar method)

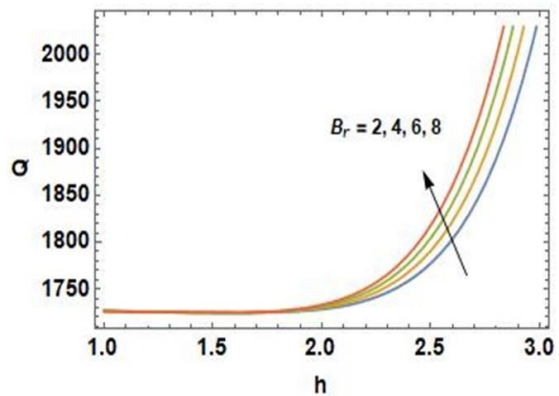


Fig. 15. Flux Q vs. radius h with local nano particle Grashof number B_r for $K = 5.26$, $A = 0.0074$, $N_b = 3$, $N_t = 5$, $G_r = 2$, $\alpha = 2.2$, $\eta = 0.8$ (Mazumdar method)

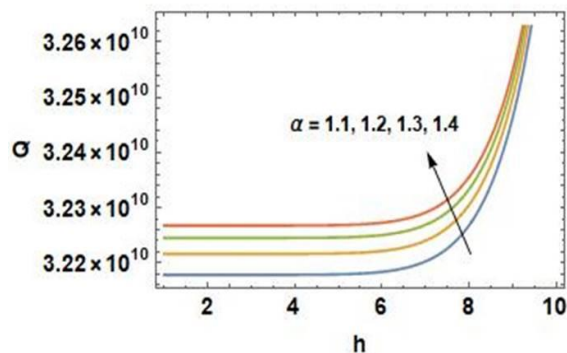


Fig. 16. Flux Q vs. radius h with couple-stress fluid parameter α for $K = 5.26$, $A = 0.0074$, $N_b = 9$, $N_t = 15$, $G_r = 6$, $B_r = 15$, $\eta = 0.8$ (Mazumdar method)

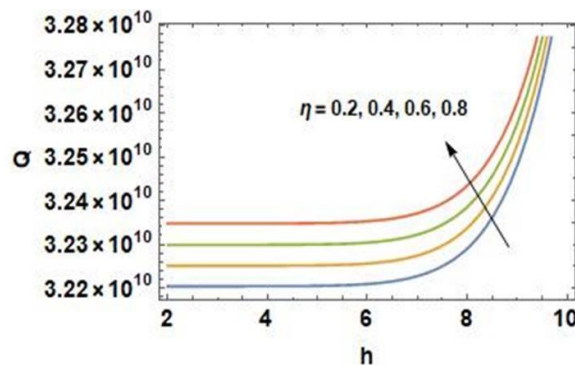


Fig. 17. Flux Q vs. radius h with couple-stress fluid parameter η for $K = 5.26$, $A = 0.0074$, $N_b = 9$, $N_t = 15$, $G_r = 6$, $B_r = 15$, $\alpha = 2.2$ (Mazumdar method)

Streamline patterns

Trapping is a fascinating occurrence of fluid movement. In other cases, the wave frame's streamlines swell to capture a bolus that flows with the wave speed as an inlet. Trapping is the process of a closed streamline producing an internally

flowing bolus. The wave pattern moves the bolus, which is defined as a capacity of fluid surrounded by closed streamlines in the wave frame. The streamlining patterns for various parameters are depicted in Figures 18-19. With increasing B_r and G_r levels, the size of the trapped bolus grows.

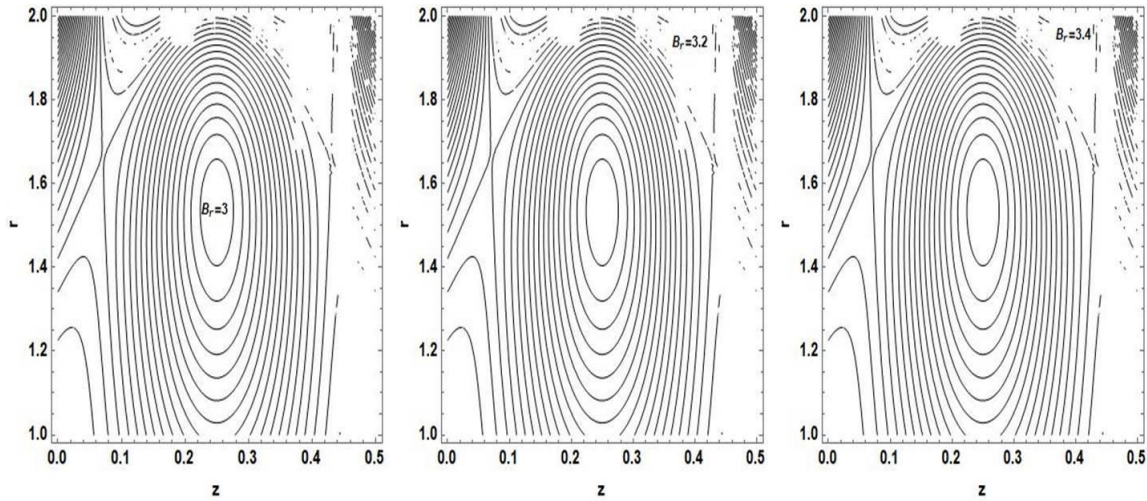


Fig. 18. Streamlines for $B_r = 3, 3.2, 3.4$

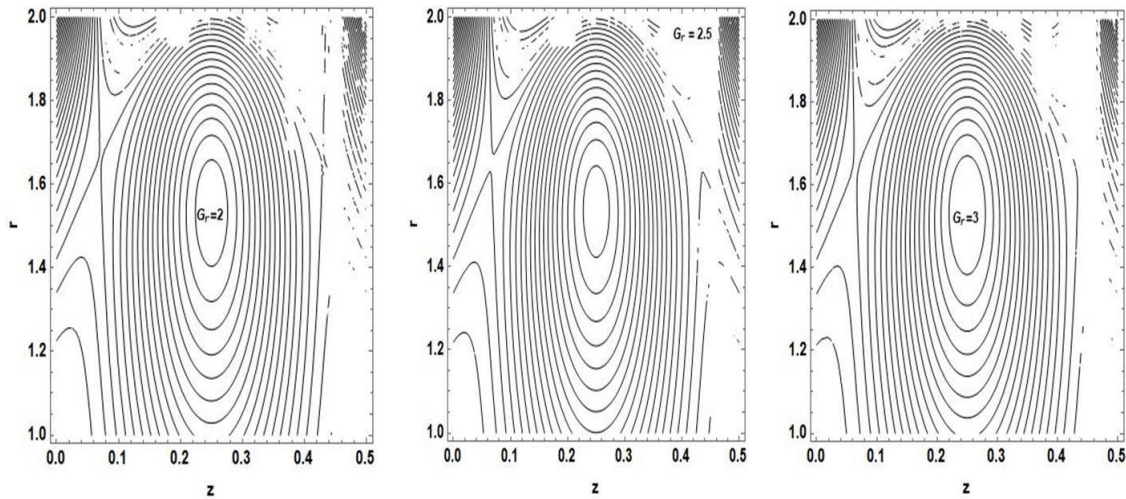


Fig. 19. Streamlines for $G_r = 2, 2.5, 3$

Conclusions

Rubinow and Keller & Mazumdar techniques are used to investigate flux variations caused by the tube's elastic nature. Graphically, the impacts of various physical factors on flux variation throughout the tube radius are examined. The following are some of the most important observations.

1. When the elastic parameters t_1, t_2, K & A are increased, the flux increases.
2. Flux grows as G_r, B_r , and couple-stress fluids increase in value.
3. As N_b and N_t increase, the flux of a couple-stress fluid in an elastic tube with peristalsis falls.
4. The size of the confined bolus grows as G_r and B_r increase.

References

- [1] Latham TW, fluid motion in a peristaltic pump, MS. Thesis, Massachusetts Institute of Technology, Cambridge (1996).
- [2] Maruthi Prasad K, Ramana Murthy JV, VK Narla. Unsteady Peristaltic Transport in Curved Channels. *Physics of Fluids*, DOI:10.1063/1.4821355, 25 (2013) 091903.
- [3] Maruthi Prasad. K, Subadra. N, Srinivas. M. A. S, Study of Peristaltic Motion of Nanoparticles of a Micropolar Fluid with Heat and Mass Transfer Effect in an Inclined Tube. *International Conference on Computational Heat and Mass Transfer*, 127, 694-702, 2015.
- [4] B.B. Divya, G. Manjunatha, C. Rajashekar, Hanumesh Vaidya, K.V. Prasad. Impact of Variable Liquid Properties on Peristaltic Mechanism of Convectively Heated Jeffrey Fluid

- in a Slippery Elastic Tube. *12(15)*, 2151-8629, 2019.
- [5] R. Ravikumar, G. Arul Freeda Vinodhini, J. Prakash, Heat Transfer and Slip Effects on the MHD Peristaltic Flow of Viscous Fluid in a Tapered Microvessels: Application of Blood Flow Research, *International Journal of Engineering and Advanced Technology (IJEAT)*, *9(1)*, 2249 – 8958, 2019.
- [6] Gudekote, M. ., & Choudhari, R., Slip Effects on Peristaltic Transport of Casson Fluid in an Inclined Elastic Tube with Porous Walls, *Journal of Advanced Research in Fluid Mechanics and Thermal Sciences*, *43(1)*, 67–80, 2020.
- [7] Choi SUS. Enhancing Thermal Conductivity of Fluids with Nanoparticles, In Signer DA, Wang HP (eds) Developments and applications of Non-Newtonian flows. *ASME, New York*, *66*, 99-105, 1995.
- [8] Noreen Sher Akbar and S. Nadeem, Peristaltic Flow of a Micropolar Fluid with Nanoparticles in Small Intestine. *Applied Nanoscience*, *3(6)*, 461-468. 2013.
- [9] K. Maruthi Prasad, N. Subadra, M. A. S. Srinivas. Peristaltic Transport of a Nanofluid in an Inclined Tube. *American Journal of Computational and Applied Mathematics*, *5(4)*, 117-128, 2015
- [10] C. Haseena, A. N. S. Srinivas, C. K. Selvi, S. Sreenadh, and B. Sumalatha, The Influence of elasticity on Peristaltic Flow of Nanofluid in a Tube, *American Scientific Publishers*, *10*, 590-599, 2021.
- [11] A. M. Abd-Alla, Esraa N. Thabet, F.S. Bayones, Numerical Solution for MHD Peristaltic Transport in an Inclined Nanofluid Symmetric Channel with Porous medium, *Scientific reports*, *12*, 3348, 2022.
- [12] Maruthi Prasad. K, Subadra. N, Mahabaleswar. U. S, Peristaltic Transport of a Couple-Stress Fluid with Nanoparticles in an Inclined Tube. *International Journal of Engineering Trends and Technology*, *48(7)*, 2231-5381, 2017.
- [13] C.K. Selvi, A.N.S. Srinivas. Peristaltic Transport of Herschel-Bulkley Fluid in a Non-Uniform Elastic Tube. *8(3)*, 253-262, 2018.
- [14] Srinivas Jangili, Samuel Olumide Adesanya, Ogunseye Abiodun Hammed, Ramoshweu Solomon Lebelo, Couple-Stress fluid flow with variable properties: A second law analysis. *Mathematical methods in the Applied Sciences*, *42*, 9-10, 2019.
- [15] M. Y. Rafiq, Z. Abbas, M. Z. Ullah, Peristaltic mechanism of couple stress nanomaterial in a tapered channel , *Ain Shams Engineering Journal*, *13*, 101779, 2022.
- [16] C. K. Selvi, A. N. S. Srinivas. The Effect of Elasticity on Bingham Fluid Flow in a Tube. *Int. journal of Mechanical Engineering and Technology*, *8(8)*, 554-564, 2017.
- [17] B. Sumalatha and S. Sreenadh, Poiseuille flow of a Jeffrey Fluid in an Inclined Elastic Tube. *Int. journal of Eng. Sciences & Research Technology*, *7(1)*, 150-160, 2018.
- [18] C.K. Selvi, A. N. S. Srinivas and S. Sreenadh. Peristaltic Transport of a Power-Law Fluid in an Elastic Tube. *Journal of Taibah University for Science*, *12(5)*, 687-698, 2018.
- [19] C. Haseena, A. N. S. Srinivas, C. K. Selvi, S. Sreenadh, and B. Sumalatha, *The Influence of elasticity on Peristaltic Flow of Nanofluid in a Tube*, *American Scientific Publishers*, *10*, 590-599, 2021.
- [20] He JH. Homotopy Perturbation Technique. *Computer Methods in Applied Mechanics and Engineering*. *178(3-4)*, 257-262, 1999.
- [21] Mazumdar, N.J. *Biofluid Mechanics*, World Scientific, Chapter.5, Singapore. 1992.
- [22] S. I. Rubinow, Joseph B. Keller. Flow of a Viscous Fluid through an Elastic Tube with Applications to Blood Flow. *J. theor. Biol.* *35(2)*, 299-313, 1972.